4. The deacylation step in acetylcholinesterase

4.1. Introduction to acetylcholinesterase

Acetylcholinesterase (AChE, EC 3.1.1.7) is a serine hydrolase, whose main biological function is to terminate impulse transmission at cholinergic synapses by rapid hydrolysis of the neurotransmitter acetylcholine (ACh) (for reviews see Quinn[68] and Rosenberry[69]). The enzyme possesses a remarkably high activity and works close to the diffusion controlled limit. The turnover rate k_{cat} for the hydrolysis of acetylcholine in aqueous solution is about $8 \times 10^{-10} s^{-1}$,[70] whereas the overall rate is about $1.6 \times 10^{4} s^{-1}$ in the enzyme active site,[71] which corresponds to a rate enhancement in the enzyme by the factor 2×10^{13}.

The X-ray crystallographic structure of AChE[72] shows a 20 Å deep and narrow cavity, which can host the substrate ACh. It is called the "aromatic gorge", because its wall is covered by 14 highly conserved aromatic residues. The catalytic triad, consisting of Ser200, Glu327 and His440, is located at the dead end of this gorge. The cationic moiety of ACh binds to the aromatic residues Trp84 and Phe330 by cation-π interactions and to the acidic residue Glu199 by electrostatic interactions. The residues of the binding pocket interacting with the acyl part of ACh are Gly119, Trp233, Phe288, Phe290, and Phe331.[73]

The reaction of AChE follows the scheme outlined in Figure 4.1, where k_1 and k_{-1} are the rate constants for the association and dissociation of AChE with its substrates and the rates k_2 and k_3 correspond to the chemical conversion steps.

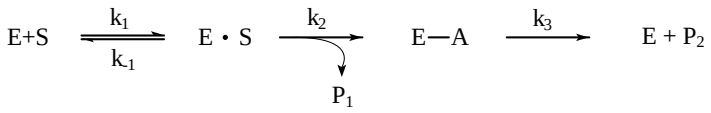

Figure 4.1.: Kinetic mechanism for ACh hydrolysis. E: AChE, S: substrate (e.g. acetylcholine), E·S: reversible enzyme substrate complex, E-A: acylated enzyme, P_1: choline, P_2: acetic acid; k_1 and k_{-1} are the rate constants for the diffusion of the substrate, k_2 and k_3 are the rate constants for the chemical conversion steps, i.e. the acylation and deacylation respectively.

The catalytic mechanism is outlined in Figure 4.2. The hydrolytic destruction of carboxyl esters, including ACh, is assumed to occur via an unstable tetrahedral intermediate (TI1) leading to a short-lived ($t_{1/2} \approx 50 \mu s$) state, where the enzyme is acylated at Ser200.[71] Subsequently, a nucleophilic attack of a water molecule occurs resulting in a second tetrahedral intermediate (TI2), which decomposes into the native enzyme and an acetate ion. This second part of the reaction is called the deacylation step and is investigated in this work. It comprises a nucleophilic attack of a water oxygen on the ester carbonyl group and a proton transfer from this water molecule to the N_ε nitrogen of the His440 side chain.

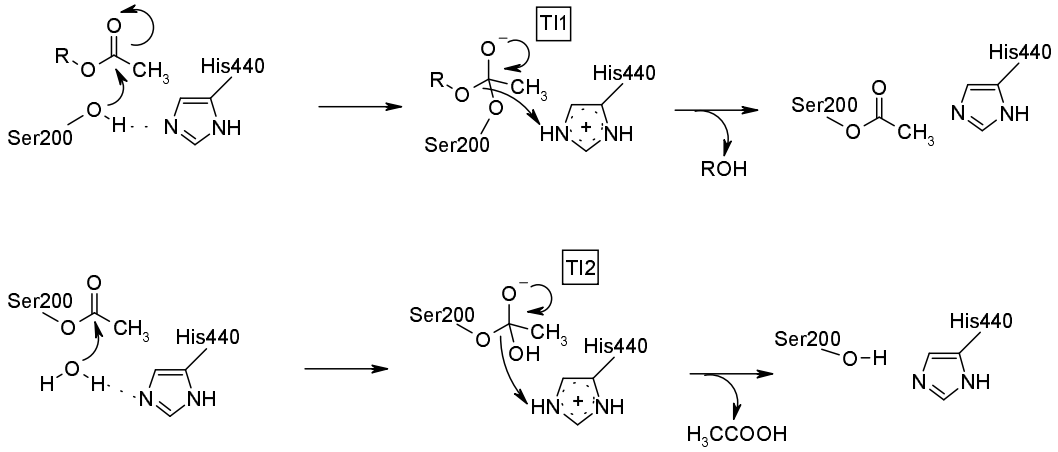

Figure 4.2.: Reaction mechanism of AChE with a carboxyl ester substrate. The top panel shows the acylation and the lower panel shows the deacylation reaction. The base in the catalytic triad is His440. Choline, the product of the acylation reaction is denoted as ROH. For both reactions, the carbonyl carbon atom of acetylcholine and Ser200 respectively proceeds from its planar geometry to a tetrahedral intermediate. (TI1 and TI2).

For the simulation of the deacylation step, the acylated enzyme is taken as the starting point. The corresponding valence bond structure I is given in Figure 4.3. The endpoint of the simulation is the tetrahedral intermediate TI2 of the deacylation step, corresponding to the valence bond structure III in Figure 4.3. As the barrier for the decomposition of the tetrahedral intermediate TI2 is lower than the barrier for its formation, the formation of this intermediate state is the rate determining step in the deacylation reaction.[74] Hence, it is sufficient to simulate the reaction up to the point, where the formation of the tetrahedral intermediate TI2 is completed.

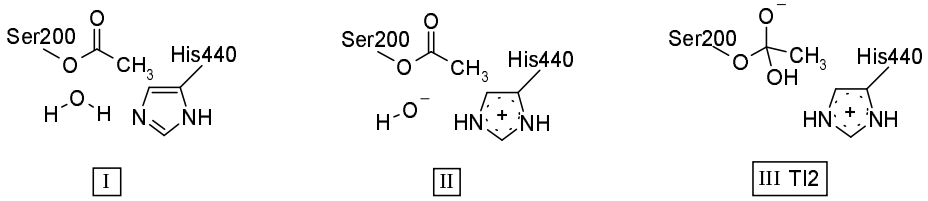

Figure 4.3.: Resonance or valence bond structures used in the EVB/FEP simulation of the deacylation step: I, II, III correspond to the reactants, the state formed after the proton transfer from water to His440 and the tetrahedral intermediate, respectively.

In crystal structures with transition state analogues of the acylation step and in modeled structures, it could be observed that the oxyanion hole in AChE, which stabilizes TI1, consists of the dipoles of the backbone NH-groups of Gly118, Gly119 and Ala201.[73,72,75,76] Glu327, as

a member of the catalytic triad, stabilizes the protonated His440. In site-directed mutagenesis studies, it was shown, that Glu327Ala and Glu327Gln mutants are inactive.[77] Furthermore, Glu199, which is located adjacent to the active site, is ascribed an important role, although it is not clear to which extent it contributes to the rate enhancement of the chemical conversion. The Glu199Gln mutant of AChE from *torpedo californica* has a k_{cat}/K_m ratio 50-fold lower than that of the native enzyme,[78] where K_m is the Michaelis constant.

Most experimental and theoretical studies on AChE focused on the diffusion of substrates to the active site or on the acylation step.[79,80,81,78] Enzymes, which by evolution are optimized for rapid catalysis, may often show similar activation barriers for the different reaction steps, since optimization requires to lower the highest barrier. Therefore, it is not surprising that for AChE, which is a very fast processing enzyme, both acylation and deacylation were found to be rate determining with a $k_{cat} = 1.6 \times 10^4 s^{-1}$.[71] For this reason I investigated the deacylation reaction, which is dramatically accelerated by the enzyme. The uncatalyzed hydrolysis of an ester, that is comparable to the acylated serine (e.g. methyl acetate), has a rate constant of $k_{cat} = 5 \times 10^{-9} s^{-1}$ in aqueous solution,[74] whereas in AChE this reaction proceeds with $1.6 \times 10^4 s^{-1}$,[71] which is as large as the overall rate of the enzyme. This is equal to an acceleration of the reaction by the factor 3×10^{12}.

The deacylation is an important process in order to understand the irreversible inhibition of AChE by compounds that modify Ser200 due to phosphorylation like sarin and soman or carbamoylation like physostigmine and epastigmine. The hydrolysis of these derivates is very slow and the understanding of the mechanism and the accelerating factors of deacylation is crucial to characterize the inhibition of AChE.[82,83]

Experimental and theoretical studies have shown that the substrates of AChE are guided into the active site gorge by a strong electrostatic monopole and dipole field.[84] This is unfavorable for the cationic product, choline, to move out of the active site after the reaction is completed.[85] Therefore, it was suggested that it may leave the active site via a "back-door",[85] but this is still a matter of debate.[86,87] To elucidate the dissociation of choline from AChE, it is important to know, at which reaction step it leaves the active site.

As outlined in chapter 2.1, the electrostatic properties of an enzyme have a significant influence on its catalytic function. Thus, in this work the protonation pattern of all titratable groups was determined in detail. This permits now to conclude how individual titratable groups stabilize the protein structure in a particular protonation state and how they reduce the energy of the transition state in an enzymatic reaction.

The present work investigates the deacylation step of AChE using computer simulation approaches. First the protonation state of the acylated enzyme is analyzed. Then the hydrolytic reaction in the active site of AChE is compared to a reference reaction in water. It is determined, how the enzyme manages to reduce the activation barrier of the reaction, three aspects deserved special attention 1) Is it possible to differentiate between a concerted or a stepwise mechanism for the proton transfer and the nucleophilic attack of the deacylation step? 2) What is the influence of choline, the product from the acylation step, on the energetics of deacylation? 3) Which protonation state of Glu199 is favorable for the stabilization of the transition state of the deacylation step?

4.2. Details of computational setup

4.2.1. The structure

The starting coordinates for the simulations were generated from the AChE crystal structure of the native enzyme from *torpedo californica* determined at 2.5 Å resolution (PDB entry 2ace).[88] This structure was solved without inhibitor and subsequently, the substrate acetylcholine was modeled into the active site using informations from a structure of AChE with the transition state analogue inhibitor m-(N,N,N-trimethylammonio)-trifluoro-acetophenone (PDB entry 1amn).[73] This model structure is believed to represent the transition state of the acylation step (TI1 in Figure 4.2). The 1amn structure is solved with a resolution of 2.8 Å only and therefore the 2ace structure was chosen as a starting point for our calculations.

The distance between the side chain oxygen of Ser200 and the carbonyl carbon of ACh is 1.4 Å. The carbon possesses a tetrahedral conformation. To obtain a model of the enzyme in its acylated form, we added the acyl part of ACh to Ser200 and deleted the coordinates of the choline part (see Figure 4.4).

Coordinates of hydrogen atoms are not available from the crystal structure. Adding hydrogen atoms to water oxygens by modeling procedures can be rather ambiguous due to the large number of possible hydrogen bonding patterns. Therefore, all waters were removed except the reactive water modeled into the structure. The electrostatic interactions of the lacking water molecules were generated by corresponding surface charges at the boundaries of the resulting cavities with a dielectric constant of $\varepsilon = 80$. For a further justification of this approach see the discussion in ref.[90] However, one water molecule plays a special role in hydrolyzing the acylated Ser200. I placed this reactive water molecule in an appropriate H-bond position to the nitrogen atom N_ε of His440. This position is also close to the carbonyl carbon atom of the acylated Ser200 (Figure 4.4).

In the X-ray structure of AChE, ten complete residues and several atoms from 23 residues are missing. I modeled and completed these residues in the structure with the program CHARMM.[91] The HBUILD command of CHARMM was used to generate the coordinates for all hydrogen atoms, leading to an all atom representation of AChE. Subsequently the whole protein was energy minimized with the CHARMM22 force field,[92] but all experimentally known atomic coordinates were fixed.

The LPBE is solved on a lattice with a finite difference method[14] implemented in the program MULTIFLEX.[93] For the protein, I started with a cubic lattice of 202.5 Å side length with 2.5 Å grid spacing centered at the geometric center of the protein. In two focusing[94] steps I reduced the side length of the cube first to 81.0 Å and then to 22.75 Å with a grid spacing of 1.0 and 0.25 Å respectively. The lattices with the higher resolution were centered on the titrating site. For the model calculation in solution, I applied lattices of 61.0 Å and 15.25 Å side length with 1.0 Å and 0.25 Å resolution.

The dielectric constant was set to $\varepsilon_p = 4$ everywhere in the protein and was set to $\varepsilon_s = 80$ in the solvent. The value of the dielectric constant in the protein is typically chosen to account for the lack of nuclear and electronic polarization effects.[1] In general the small value $\varepsilon_p = 4$ of the dielectric constant in proteins is chosen, when applying a detailed molecular charge model. Larger values of the protein dielectric constant of up to $\varepsilon_p = 20$ are chosen for cruder molecular charge models, where for instance the protonation of a titratable group is modeled simply by placing a unit charge at a central atom of the titratable site.[95,96] For the solvent, I used an ionic strength of 100 mM and an ion exclusion layer of 2.0 Å around the protein. The boundary between the protein and the solvent was established by the surface resulting from a probe, consisting of a sphere with 1.4 Å radius, rolling on the van der Waals surface of the protein and model compound,

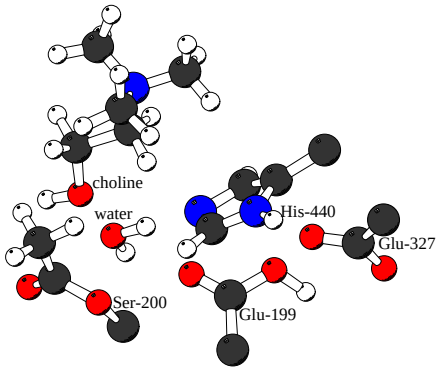

Figure 4.4.: The active site of the acylated AChE. Only the side chains of the amino acids are shown. The water molecule is modeled into the structure, such that it has an H-bond distance (2.8 Å) to the N_ε atom of His440, to which the proton is transferred during the deacylation reaction. Additionally its hydrogen atom is positioned close (3.4 Å) to the carbonyl carbon atom of the acyl group of Ser200. (Drawn with MOLSCRIPT.[89])

respectively. Cavities in the protein, which can host a sphere of radius 1.4 Å are considered to be solvent accessible and thus possess a dielectric constant of $\varepsilon_s = 80$.

The atomic partial charges of the amino acids, including the charged and neutral state of the titratable residues were taken from the CHARMM22 parameter set.[92] For some of the titratable residues (Arg, Lys, Cys) only the standard protonation state is included in this parameter set. For these residues, the atomic partial charges were calculated with the program SPARTAN[97] using the semiempirical PM3 method and the CHELPG procedure,[98] where the charges are determined such that they reproduce the electrostatic potential outside of the molecular group appropriately. The calculated charges are summarized in Appendix D.

4.2.2. Simulation conditions

The MD simulations and free energy calculations were performed with the program Q[99] using the CHARMM22 force field.[92] The starting point for the deacylation reaction was the acylated enzyme, corresponding to resonance state I in Figure 4.3. I simulated the deacylation reaction under several conditions: In one case I treated it as a two step mechanism with proton transfer and subsequent nucleophilic attack using resonance states I, II and III in Figure 4.3, where resonance state III corresponds to the tetrahedral intermediate TI2 (Figure 4.2), which is the endpoint of the simulation. In this stepwise reaction I applied the mapping potentials $\varepsilon_{map}^{I,II}(\lambda)$ and $\varepsilon_{map}^{II,III}(\lambda)$ and the electronic energy surfaces $E_g^{I,II}$ and $E_g^{II,III}$ for the proton transfer and the nucleophilic attack, respectively. Alternatively, I modeled it as a concerted mechanism, where proton transfer and nucleophilic attack proceed simultaneously with a direct transition from state I to state III by using the mapping potential $\varepsilon_{map}^{I,III}(\lambda)$ and the electronic energy surface $E_g^{I,III}$.

The partial charges for the tetrahedral intermediate TI2 in resonance structure III were calculated with a quantum chemical *ab initio* method using the 6-31G* basis set and the MK charge model[100] implemented in GAUSSIAN 98.[101] The charges are listed in Table 4.1. The titratable residues were charged according to the calculated protonation pattern.

The protein was immersed in a 23 Å sphere of TIP3P water. Water molecules whose oxygen atom had a closer contact than 2.7 Å to non-hydrogen atoms of the protein were removed. The center of the water sphere was placed at the C_γ-atom of the imidazole ring of His440 to obtain a suitable embedding of the reactive center. For non-bonded interactions we used a cutoff of 12.0 Å. Electrostatic interactions over longer distances were included by the local reaction field method.[102] Atoms, which were initially located more than 23.0 Å from the center of the molecular system, *i. e.* the C_γ atom of His440, were fixed to their crystallographic coordinates and excluded from non-bonded interactions. The waters were subjected to radial and polarization surface restraints by a surface constraint all atom solvent (SCAAS) related model.[103,104] Water bond length and angles were constrained with the SHAKE algorithm.[105]

Before MD simulations for the different λ ensembles were performed, the protein was subject to a careful structural relaxation at 30 K at the intermediate λ value $\lambda = 0.5$, which is close to the transition state. For that purpose MD simulations were applied using increasing time steps. With each of the step sizes 0.01 fs, 0.1 fs and 1.0 fs, an MD simulation of 3000 time steps was performed. Subsequently the molecular system was equilibrated at 300 K running an MD simulation for another 10000 time steps with a step size of 1.0 fs. The MD simulations for each of the reactions were started with $\lambda = 0.5$ and proceeded towards the products ($\lambda = 1.0$) and the reactants ($\lambda = 0.0$). To accomplish an efficient sampling, λ was varied in steps of 0.1 within the interval $\lambda \in [0.1, 0.9]$ and in steps of 0.02 within the end intervals $\lambda \in [0, 0.1]$ and $\lambda \in [0.9, 1.0]$. Each λ ensemble generated, comprised an MD trajectory of 4 ps. The data of the first 0.5 ps of each λ ensemble were used for equilibration and discarded. The parameters used for the MD simulation and the EVB method are summarized in Table 4.2.

4.3. Results and Discussion

4.3.1. The protonation state

I calculated the protonation pattern of the acylated and the free enzyme using a continuum electrostatic method. In both cases, I found the same six residues in a non standard protonation state: Asp392, Glu199, Glu278 and Glu445 were uncharged and His471 and His513 were positively charged. However, the acidic side chains of Asp392, Glu278 and Glu445 are located more than

residue	atom	I	II	III
Ser-200	CB	-0.110	-0.110	0.058
	HB1	0.120	0.120	0.011
	HB2	0.120	0.120	0.011
	OG	-0.340	-0.340	-0.519
	CD	0.630	0.630	1.096
	OD	-0.520	-0.520	-0.943
	CT	-0.170	-0.170	-0.663
	HT1	0.090	0.090	0.090
	HT2	0.090	0.090	0.090
	HT2	0.090	0.090	0.090
Water	OH	-0.834	-1.010	-0.799
	H1	0.417	0.440	0.440
	H2	0.417	0.010	0.379
His-440	CB	-0.090	-0.050	-0.050
	CB1	0.090	0.090	0.090
	CB2	0.090	0.090	0.090
	CG	-0.050	0.190	0.190
	ND1	-0.360	-0.510	-0.510
	HD1	0.320	0.440	0.440
	CE1	0.250	0.320	0.320
	HE1	0.130	0.180	0.180
	NE2	-0.700	-0.510	-0.510
	CD2	0.220	0.190	0.190
	HD2	0.100	0.130	0.130

Table 4.1.: EVB atomic charges in units of an elementary charge. The charges of state I are taken from the CHARMM22 force field, the charges of the OH^- ion are from Åqvist[8] and the charges for the tetrahedral intermediate in state III are calculated with a quantum chemical ab initio method as explained in the text.

11 Å away from His440 in the active site. The two doubly protonated histidines are more than 20 Å away from the active site. Hence, these residues are not supposed to have a significant influence on the catalytic reaction. Whereas Glu199, which is highly conserved in AChE from several species, is located close to the active site. The distances of the two carboxylate oxygens to the nitrogen atom N_ε of His440 are only 5.4 Å and 4.4 Å respectively. The energy required to deprotonate Glu199, which in the equilibrium state is protonated, is 3.8 kcal/mol for the acylated and 2.6 kcal/mol for the free enzyme, both without choline. This energy difference refers to a protonation state, where all other titratable groups are in equilibrium.

4.3.2. Reference reaction in solution

To clarify the effect of the enzyme environment on the ester hydrolysis, a reference reaction to calibrate the EVB-parameters is needed (see chapter 3.3). As indicated above, the hydrolysis of the acetylated Ser200 can be considered as a two step process: 1.) a proton transfer reaction from a water molecule to His440 and 2.) a nucleophilic attack of the resulting hydroxide ion on the carbonyl carbon atom of the ester leading to a tetrahedral intermediate TI2. The energy

Morse	$\Delta M(b) = D_M(1-exp(-\mu(b-b_0))^2$
O-H	$D_M = 110.0, b_0 = 1.00, \mu = 2.00$
N-H	$D_M = 98.3, b_0 = 1.10, \mu = 2.00$
O-C	$D_M = 92.0, b_0 = 1.43, \mu = 2.00$
repulsive	$V_{rep} = C_{ij}e^{-ar}$
O$\cdots$H	$C_{ij} = 1950.0, a = 4.2$
N$\cdots$H	$C_{ij} = 150.0, a = 2.5$
C$\cdots$O	$C_{ij} = 65.0, a = 2.5$
EVB parameters	
proton transfer	$A = 18.5, \mu = 0.0, \eta = 0.4, r^{\ddagger}_{XY} = 2.1$
	$\alpha = 119.0$
nucleophilic attack	$A = 66.5, \mu = 0.0, \eta = 0.02, r^{\ddagger}_{XY} = 2.9$
	$\alpha = 241.0$
concerted reaction	
set 1	$A = 69.9, \mu = 0.0, \eta = 0.00, r^{\ddagger}_{XY} = 0.0$
	$\alpha = 371.7$
concerted reaction	
set 2	$A = 82.9, \mu = 0.0, \eta = 0.00, r^{\ddagger}_{XY} = 0.0$
	$\alpha = 374.4$

Table 4.2.: EVB interaction parameters (in kcal/mol and Å). The Morse potential parameters and the repulsive potentials for N$\cdots$H and C$\cdots$O are taken from Warshel.[45] The interaction for O$\cdots$H is adjusted such, that the repulsive potential has the same r^{-12} dependence as the repulsive part of the Lennard Jones interaction, but shifted to smaller distances by around 0.5 Å.

difference in units of kcal/mol between the product and reactant state of the proton transfer reaction in water can be estimated using the relevant pK_a values:

$$\begin{aligned} \Delta G^{water}_{PT} &= 1.38[pK_a(H_2O) - pK_a(HisN_\varepsilon)] \\ &= 1.38(15.7 - 6.6) = 12.6 \end{aligned} \tag{4.1}$$

The pK_a value of histidine is taken from Ullmann and Knapp[1] and the value of water is calculated using the Henderson Hasselbalch equation for the decomposition of water: $pK_a(H_2O) = pH - log\frac{[OH^-]}{[H_2O]}$ and taking pH = 7.0, [OH^-] = 10^{-7} mol/l and [H_2O] = 55.5 mol/l, yielding pK_a(H_2O)=15.7.

With the known difference of pK_a values of the reacting fragments in aqueous solution, the corresponding activation barrier $\Delta G^{\ddagger}$ of the proton transfer reaction can be deduced from a linear free energy relationship (LFER). For the LFER evaluation, I make the assumption that the reverse reaction of our proton transfer reaction is diffusion controlled and has a rate constant of $10^{10} mol^{-1}s^{-1}$.[106] With the known difference of pk_a values one obtains the rate constant k of the proton transfer from $log10^{10} - logk = \Delta pK$ as $k = 7.9\ M^{-1}s^{-1}$. With the use of the Arrhenius rate law according to $k = 10^{13}s^{-1}e^{-\Delta G/RT}$ we obtain the corresponding energy barrier, which is 16.3 kcal/mol.

For the nucleophilic attack reaction, we used experimental data of a base catalyzed hydrolysis of methyl acetate.[74] The activation barrier of forming the tetrahedral intermediate in the hydrolysis reaction of methyl acetate is found to be 18.5 kcal/mol and the free reaction energy is 10.0 kcal/mol.[74] From transition state theory, one obtains for this energy barrier a rate constant of $k = 1.52 \times 10^{-1} M^{-1} s^{-1}$, which refers to a 1 M solution of OH^-. Hence, the rate constant for OH^- and methyl acetate in the same solvent cage would be $55.5M \times 1.52 \times 10^{-1} M^{-1} s^{-1} = 8.36 s^{-1}$ leading to an activation barrier of 16.6 kcal/mol.

With the energetics of the stepwise mechanism, the overall activation barrier of the reference reaction adds up to 12.6 kcal/mol + 16.6 kcal/mol = 29.2 kcal/mol and the overall free reaction energy is 12.6 kcal/mol + 10.0 kcal/mol = 22.6 kcal/mol, which is however not measurable, since the the tetrahedral intermediate is not stable and decays spontaneously. The schematic energy profile of the stepwise reaction can be seen in Figure 4.5a. Alternatively, the actual reaction may proceed in a concerted mode. Since the concerted reaction type may implicitly involve also aspects of the sequential reaction mechanism, it should normally result in a lower activation barrier for the reaction in the solvent and in the enzyme. Also the concerted mechanism requires a suitable calibration of the EVB parameters describing the reaction in the solvent. However, there is no experimental model system available to perform a straightforward calibration for this mechanism. Therefore, I consider two parameter sets to see how the rate enhancement depends on the choice of EVB parameters (see Table 4.2). The first parameter set is designed to yield the same value for the overall energy barrier (29.2 kcal/mol) and the reaction energy (22.6 kcal/mol) as the two step reaction mechanism in aqueous solution. This parameter set can be considered as an upper limit, where the activation barrier is as large as for the sequential reaction mechanism in aqueous solution. With the second parameter set I model an activation barrier, which in water is reduced by 5 kcal/mol yielding a value of 24.2 kcal/mol. The overall free reaction energy is of course the same in the stepwise and the concerted mechanism. The schematic profile of the concerted mechanism with parameter set 2 can be seen in Figure 4.5b. The reduced activation barrier of 24.2 kcal/mol from parameter set 2 is close to the conceivable lower limit, which should be equal to the reaction energy of 22.6 kcal/mol.

4.3.3. EVB/FEP calculations

The EVB calculations were carried out using different simulation conditions. The deacylation reaction was simulated as a two step mechanism and as a concerted mechanism. Additionally, both mechanisms were investigated with choline absent or in the binding pocket. To check the influence of Glu199, the concerted reactions with choline in the binding pocket were also simulated with this glutamate in the charged, unprotonated state, albeit, according to our computations of electrostatic energies, the unprotonated Glu199 would not be appropriate, since this state possesses a 3.8 kcal/mol higher energy (see chapter 4.3.1). The calculated values of the free reaction energies and activation barriers are summarized in Table 4.3. The free energy profiles of the reactions in water and in the enzyme are given in Figure 4.7 explicitly and in Figure 4.5 schematically.

Stepwise mechanism

The free energy profile of the proton transfer reactions in Figure 4.7a shows that the corresponding reaction rate is practically not enhanced by the enzyme. The activation barrier is reduced by only 0.9 kcal/mol and 2.0 kcal/mol in the absence and presence of choline respectively compared to the reference reaction in water. The free reaction energies of the proton transfer in the enzyme

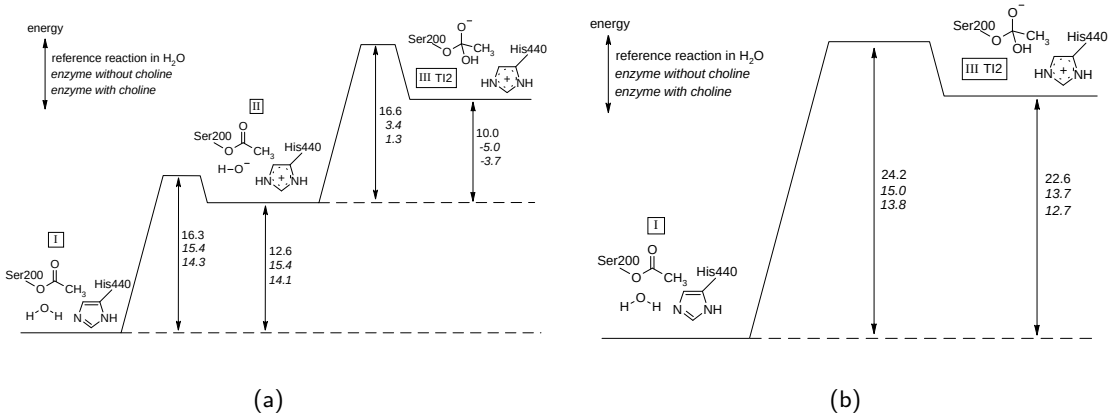

Figure 4.5.: Schemes of the free energy profiles of the stepwise mechanism (a) and the concerted mechanism with EVB parameter set 2 (b) for the reference reaction in water and for the catalyzed reactions. The three numbers besides the arrows refer from top to bottom to the reference reaction in water, the reaction in AChE without choline and with choline in the binding pocket respectively. All energies are given in kcal/mol.

are even increased by 2.8 kcal/mol and 1.5 kcal/mol as compared to aqueous solution. This indicates that the proton transfer reaction is not favored by the enzyme. The role of the enzyme to enhance the overall rate of the stepwise mechanism results from the considerable decrease of the activation barrier and the free reaction energy of the nucleophilic attack reaction only (see Figure 4.7b and 4.5a). In the absence and presence of choline the nucleophilic attack reaction has activation barriers that are 15.0 kcal/mol and 13.7 kcal/mol lower than the corresponding value of the reference reaction, respectively. The corresponding free reaction energies are negative and lowered by 13.2 kcal/mol and 15.3 kcal/mol as compared to the reference reaction.

Concerted mechanism

The simulation of the concerted reaction with the EVB parameter set 1, that corresponds to the energetics of a stepwise mechanism (see chapter 4.3.2) yielded an energy profile (Figure 4.7c) that is very similar to the overall energy profile of the stepwise reaction. To obtain the total activation barrier for the stepwise reactions, the free reaction energy ΔG of the proton transfer reaction and the activation energy $\Delta G^{\ddagger}$ of the nucleophilic attack reaction have to be summed up. This leads to $\Delta G^{\ddagger}_{total} = 18.8$ kcal/mol and $G^{\ddagger}_{total} = 15.4$ kcal/mol for the stepwise reactions in the absence and presence of choline respectively (see Figure 4.5a). Comparing these energies with the corresponding energies of the concerted reaction obtained with the EVB parameter set 1 (18.3 kcal/mol and 17.0 kcal/mol, Table 4.3) it can be seen, that the corresponding differences are only 2% and 9% respectively. This indicates that the enzyme accelerates the stepwise and the concerted reaction similarly. Hence, using the same parameterization for the reference reaction of the concerted and the stepwise mechanism one cannot decide, which mechanism is prevailing. Anyhow, the enzyme without choline in the binding pocket lowers the activation barrier of the total reaction by 40 % compared to the reaction in water, corresponding to a rate enhancement

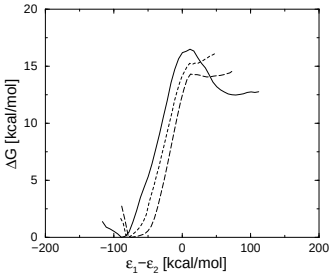

(a) Proton Transfer

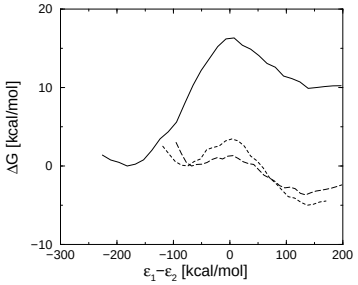

(b) Nucleophilic Attack

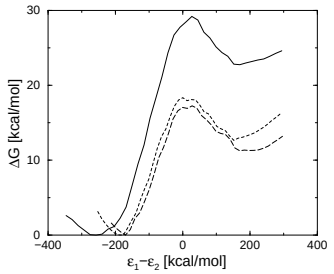

(c) Concerted Reaction 1

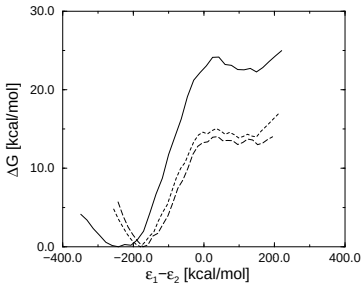

(d) Concerted Reaction 2

Figure 4.6.: Free energy profiles for the proton transfer, the nucleophilic attack and the concerted reactions with the EVB parameter set 1 and 2. The solid line curves show the energy profiles of the calibrated reference reactions in water. The two other curves denote the reactions in the enzyme (dotted: without choline, dashed: with choline). All enzymatic free energy profiles are from simulations with uncharged Glu-199.

Reaction	ΔG	$\Delta G^{\ddagger}$	$(\Delta\Delta G)^{w\rightarrow p}$	$(\Delta\Delta G^{\ddagger})^{w\rightarrow p}$
PT no choline	15.4	15.4	+2.8	-0.9
PT with choline	14.1	14.3	+1.5	-2.0
NA no choline	-5.0	3.4	-15.0	-13.2
NA with choline	-3.7	1.3	-13.7	-15.3
CONC no choline [1]	12.8	18.3	-9.8	-10.9
CONC with choline [1]	11.3	17.0	-11.3	-12.2
CONC no choline [2]	13.7	15.0	-8.9	-9.2
CONC with choline [2]	12.7	13.8	-9.9	-10.4

Table 4.3.: Results of free energy perturbation: Free energies of the enzymatic reactions; PT: proton transfer, NA: nucleophilic attack, CONC: concerted reaction. The concerted reactions were simulated using two different EVB-parameter sets (see Table 4.2). The numbers in square brackets behind the reaction type denote the used set. The superscript $w \rightarrow p$ denotes the difference in free energy between the reaction in water and the reaction in the enzyme, where $\Delta\Delta G^{w\rightarrow p} = \Delta G_{protein} - \Delta G_{water}$. Energies are given in kcal/mol.

by the factor $\sim 10^8$. In the presence of choline this value increases to 42 % corresponding to a rate enhancement by the factor $\sim 10^9$ compared to the reaction in water.

With the EVB parameter set 2, the enzyme diminishes the activation barrier by the same amount with respect to the reference reaction as by using parameter set 1 (see Figure 4.7 and 4.5b). This indicates, that the calculated stabilization of the transition state in the enzyme is not very sensitive on the exact calibration of the EVB parameters. The energy barriers obtained with the parameter set 2 are 15.0 kcal/mol without choline and 13.8 with choline. The latter value is close to the experimentally found value of 12.0 kcal/mol.[71]

Comparison of rate constants

The rate constant calculated with parameter set 2 and choline in the binding pocket is $k = 5.6 \times 10^2 s^{-1}$ and thus, only by a factor 29 smaller than the corresponding experimental value that is $k = 1.6 \times 10^4 s^{-1}$. Compared to the reference reaction, this is a rate enhancement of about the factor 10^7. Without choline in the binding pocket the rate constant is $k = 74 s^{-1}$. This value is by the factor 2.2×10^2 smaller then the experimental value. Using parameter set 1 with choline in the binding pocket the rate constant amounts to $k = 2.6 s^{-1}$ and is thus by the factor 6×10^3 smaller than the corresponding experimental value. Without choline in the binding pocket the calculated rate constant is $k = 0.3 s^{-1}$. This is by a factor of 5.4×10^4 smaller than the experimental rate constant. The rate constants of the stepwise mechanism with and without choline in the binding pocket are of the same magnitude as those of the concerted mechanism with parameter set 1. Hence, regarding the rate of the deacylation reaction in AChE, only the concerted mechanism with the EVB parameter set 2 can explain the experimental values satisfactorily.

Role of specific residues

The MC titration of the acylated enzyme resulted in an uncharged Glu199 and a charged Glu327. The role of Glu199 was discussed in several previous experimental and theoretical works. In site-directed mutagenesis studies it was found, that the Glu199Gln mutant showed only a 5-fold decrease in k_{cat}.[107,108] It was shown,[79] that the negative charge of Glu199 has only a moderate

accelerating effect on the acylation step. On the other hand it was stated from theoretical calculations that Glu199 should have a negative charge and removing this charge would result in a 32-fold reduction of the acylation rate.[80]

The aging reaction or dealkylation of phosphonylated AChE can be compared with the deacylation reaction. The starting point of the aging reaction is a phosphonylated Ser200 that undergoes a dealkylation, which is catalyzed by the enzyme. From mutation studies it was concluded, that Glu199 should be deprotonated during the aging reaction.[109] This makes it likely that also the acylated enzyme should have Glu199 in the charged state. The reactant state of the aging reaction is a neutral phosphonyl derivate of Ser200, which should have a comparable electrostatic effect as the acyl group of the acylated intermediate. Thus the experimental information from the aging reaction contradicts the result from our theoretical titration. It should be mentioned, however, that two features of the aging reaction differ from the deacylation reaction: a) His440 is assumed to be doubly protonated in the reactant state of the aging reaction. Thus, considering the electrostatic potential in the active site, the negative charge state of Glu199 would be favoured. b) Furthermore in the aging reaction a carbenium ion intermediate occurs, which profits from stabilization by a negatively charged Glu199.

In our EVB/FEP calculation of the deacylation reaction in AChE, I found that a negative charge at Glu199 increases the activation barrier of the deacylation step from 13.8 kcal/mol to 19.7 kcal/mol in the absence of choline in the binding pocket. Hence, for a negatively charged Glu199 the rate enhancement compared to the reference reaction is a factor of 10^3 only. From this large effect and from the titration calculation, I conclude that Glu199 has to be uncharged and a mutation to Gln should consequently have only a small effect on the rate of the deacylation reaction. This is in agreement with mutation studies in decarbamoylation reactions of irreversibly inhibited AChE, where the barrier of the decarbamoylation reaction did not vary with the Glu199Gln mutation.[78]

The EVB/FEP simulation showed, that AChE reduces the activation barrier of the deacylation reaction considerably compared with the reaction in water. Glu327 with its negative charge contributes to the stabilization of the positively charged histidinium ion. The distance between the carboxylate oxygen of Glu327 and the nitrogen atom N_δ of His440 is 2.6 Å. Hence, there is a strong hydrogen bond. In analogy to the stabilization of the tetrahedral intermediate TI1 in the acylation reaction, in the deacylation reaction the tetrahedral intermediate TI2 is stabilized similarly with the amide groups of Gly118, Gly119 and Ala201 forming the oxyanion hole. The amide nitrogen atoms of these three residues are located 2.7 Å, 2.7 Å and 2.8 Å respectively from the carbonyl oxygen atom in the tetrahedral intermediate TI2. The structure of the tetrahedral intermediate and the stabilizing NH dipoles are visualized in Figure 4.7.

Choline

The influence of choline on the activation barrier of the deacylation reaction is not large. In the concerted mechanism, I found that the presence of choline accelerates the reaction by the factor 10. This effect is too small to decide, whether the choline is released before or after the deacylation reaction. It can merely be deduced that the presence of choline does not hinder the deacylation reaction. Hence, the release of the first product, the choline, may occur before or after deacylation. However, in the latter case, choline could leave the binding pocket together with the acetate ion as a neutral ion pair, which would be energetically more favorable. This could solve the problem that the positively charged acetylcholine binds very well at its binding site in the enzyme via strong cation-π-interactions with Trp-84 and Phe-330 rendering the release of choline alone to be unfavorable. The neutralized positive charge of choline would facilitate its removal from the

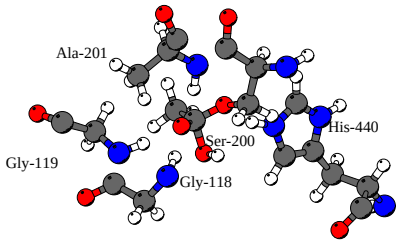

Figure 4.7.: Tetrahedral intermediate TI2 in the deacylation step. The negatively charged tetrahedral intermediate is stabilized by the NH dipoles of the backbone amide groups of Gly118, Gly119 and Ala201 (depicted in black). These dipoles constitute the so called oxyanion hole. This is an averaged structure from a trajectory of an MD simulation for the product ensemble $\lambda = 1.0$, which contains the tetrahedral intermediate TI2. Drawn with MOLSCRIPT.[89]

binding pocket in AChE by weakening the cation-π interaction with the aromatic residues and the electrostatic interactions with the negatively charged groups inside the binding pocket. Though, from experimental studies on the noncompetetive inhibition of AChE by thiocholine, which has comparable binding affinities as choline, a rate of $\sim 10^5 s^{-1}$ for the release of thiocholine from AChE was deduced.[110,111] This process is faster than the deacylation, suggesting that choline leaves the binding pocket before deacylation. For a quantitative investigation of the interaction between choline and enzyme the cation-π interaction between choline and the aromatic residues in the binding pocket must be considered.[112,113] This is not possible with the force field used at present and is therefore out of the scope of this study.

4.4. Conclusion

The Monte Carlo titration calculation, based on electrostatic energies obtained by solving the LPB equation, resulted in a protonated Glu199 in the acylated as well as in the free enzyme state. Deprotonating Glu199, while all other groups can adopt their equilibrium protonation state, results in an energy increase of 3.8 kcal/mol and 2.6 kcal/mol for the acylated and the free enzyme state respectively. The simulation of the deacylation step using the EVB method lead to an energy barrier of the deacylation step in AChE that is decreased by 11-12 kcal/mol as compared to a corresponding reference reaction in water. This is equivalent to a rate enhancement of about the factor 10^7. With Glu199 deprotonated, the rate enhancement was 10^3 only. I obtained the largest rate constant of the deacylation reaction with choline inside the binding pocket using a concerted reaction mechanism with EVB parameter set 2. The corresponding rate constant is $k = 5.5 \times 10^2 s^{-1}$. The experimental value of $1.6 \cdot 10^4 s^{-1}$ is only by a factor of 29 larger than the calculated value.

By simulating the deacylation reaction, I observed that the tetrahedral intermediate TI2, which occurs during this reaction, is stabilized by three dipoles from the protein backbone NH groups of Gly118, Gly119 and Ala201. In the acylation reaction of AChE these residues form the so called oxyanion hole. Thus, these residues have a similar function in the acylation and deacylation reaction. Glu327, which belongs to the catalytic triad of AChE, forms an H-bond with His440 and thus stabilizes the positive charge of the imidazole ring, which occurs during the deacylation reaction.

I considered that choline, the reaction product of the acylation step, may still be present in the binding pocket during deacylation, albeit experiments support an earlier release. In my simulations the choline did not have a significant influence on the energy barrier of the deacylation reaction. Hence, it is not possible to conclude from the present computations, which concentrate on transition state stabilization by the enzyme environment, at which reaction step, before or after the deacylation, choline leaves the binding pocket.